

## SUPPLEMENTAL INFORMATION

### Multimodal tracking of (controlled) *Staphylococcus aureus* infections in mice

Mick M. Welling<sup>a#</sup>, Clarize M. de Korne<sup>a,c</sup>, Silvia. J. Spa<sup>a</sup>, Danny M. van Willigen<sup>a</sup>, Albertus W. Hensbergen<sup>a</sup>, Anton Bunschoten<sup>a,b</sup>, Nikolas Duszenko<sup>a,c</sup>, Wiep Klaas Smits<sup>d</sup>, Meta Roestenberg<sup>c</sup>, Fijis W. B. van Leeuwen<sup>a,b</sup>

<sup>a</sup> Interventional Molecular Imaging Laboratory, Department of Radiology, Leiden University Medical Center, Leiden, the Netherlands

<sup>b</sup> Laboratory of BioNanoTechnology, Department of Agrotechnology and Food Sciences, Wageningen University & Research, Wageningen, the Netherlands

<sup>c</sup> Department of Parasitology and Department of Infectious Diseases, Leiden University Medical Center, Leiden, the Netherlands

<sup>d</sup> Department of Medical Microbiology, Section Experimental Bacteriology, Leiden University Medical Center, Leiden, the Netherlands

# Corresponding author; Mick M. Welling, E-mail: [m.m.welling@lumc.nl](mailto:m.m.welling@lumc.nl)

Page S1: Title page

Page S2: Table S1

Page S3: Figure S1

Page S4: Figure S2

Page S5: Figure S3

Page S6: Figures S4a & b

Page S7: Figure S5

Page S8: Figure S6

Page S9: Figure S7

Page S10: Figure S8a-c

Page S11: Figure S9a-d

**Table S1.** The biodistribution of I.M. administered  $^{99m}\text{Tc}$ -UBI<sub>29–41</sub>-Cy5-N3 labelled *S. aureus*.

Data (expressed as the mean  $\pm$  SD of the percentage of the injected dose per gram tissue (%ID/g) of 3 observations) were calculated based on the radioactive counts measured in various tissues at 4 h, 20 h, and 28 h post-injection of the radioactive tracer.

Tissue	%ID/g		
	4 h p.i.	20 h p.i.	28 h p.i.
Blood	1.98 $\pm$ 0.53	0.15 $\pm$ 0.11	0.13 $\pm$ 0.03
Thyroid gland	1.37 $\pm$ 0.32	0.79 $\pm$ 1.07	1.14 $\pm$ 0.66
Salivary gland	6.12 $\pm$ 1.23	3.36 $\pm$ 5.09	2.51 $\pm$ 1.90
Heart	0.83 $\pm$ 0.16	0.46 $\pm$ 0.70	0.37 $\pm$ 0.25
Lungs	1.40 $\pm$ 0.37	0.59 $\pm$ 0.91	0.40 $\pm$ 0.30
Bladder	82.06 $\pm$ 33.50	10.85 $\pm$ 15.04	3.64 $\pm$ 2.70
Liver	8.75 $\pm$ 1.09	4.77 $\pm$ 6.33	4.15 $\pm$ 3.74
Spleen	0.89 $\pm$ 0.33	0.86 $\pm$ 1.37	1.19 $\pm$ 0.47
Kidneys	33.67 $\pm$ 6.30	11.26 $\pm$ 16.72	8.67 $\pm$ 7.61
Stomach	3.90 $\pm$ 4.66	2.93 $\pm$ 4.07	2.87 $\pm$ 2.25
Intestines	17.90 $\pm$ 14.05	1.43 $\pm$ 1.69	1.96 $\pm$ 0.72
Infected muscle	51.91 $\pm$ 19.53	42.12 $\pm$ 21.52	44.44 $\pm$ 25.70
Control muscle	0.66 $\pm$ 0.21	0.63 $\pm$ 0.42	1.38 $\pm$ 1.33
Brains	0.13 $\pm$ 0.04	0.06 $\pm$ 0.08	0.08 $\pm$ 0.03
Excretion (%ID; cumulative)	42.90 $\pm$ 22.47	78.21 $\pm$ 8.33	83.16 $\pm$ 8.32
Infection-to-blood ratio	27.99 $\pm$ 13.17	301.20 $\pm$ 120.83	359.20 $\pm$ 227.78
Control-to-blood ratio	0.35 $\pm$ 0.15	4.23 $\pm$ 2.51	9.76 $\pm$ 7.84

**Figure S1.** Chemical synthesis pathway of UBI<sub>29-41</sub>-Cy5-N<sub>3</sub>. **a)** NaN<sub>3</sub>, DMF, 50°C; **b)** 6-bromohexanoic acid, CH<sub>3</sub>CN, 60°C; **c)** CH<sub>3</sub>CN, 55°C; **d)** DiPEA, Ac<sub>2</sub>O, CH<sub>2</sub>Cl<sub>2</sub>, 0 °C to R.T.; **e)** NaOAc, EtOH, R.T.; **f)** HSPyU, DiPEA, DMSO, R.T.; **g)** UBI<sub>29-41</sub>, 0.1M phosphate buffer pH 8.5/DMSO 3:1, R.T.

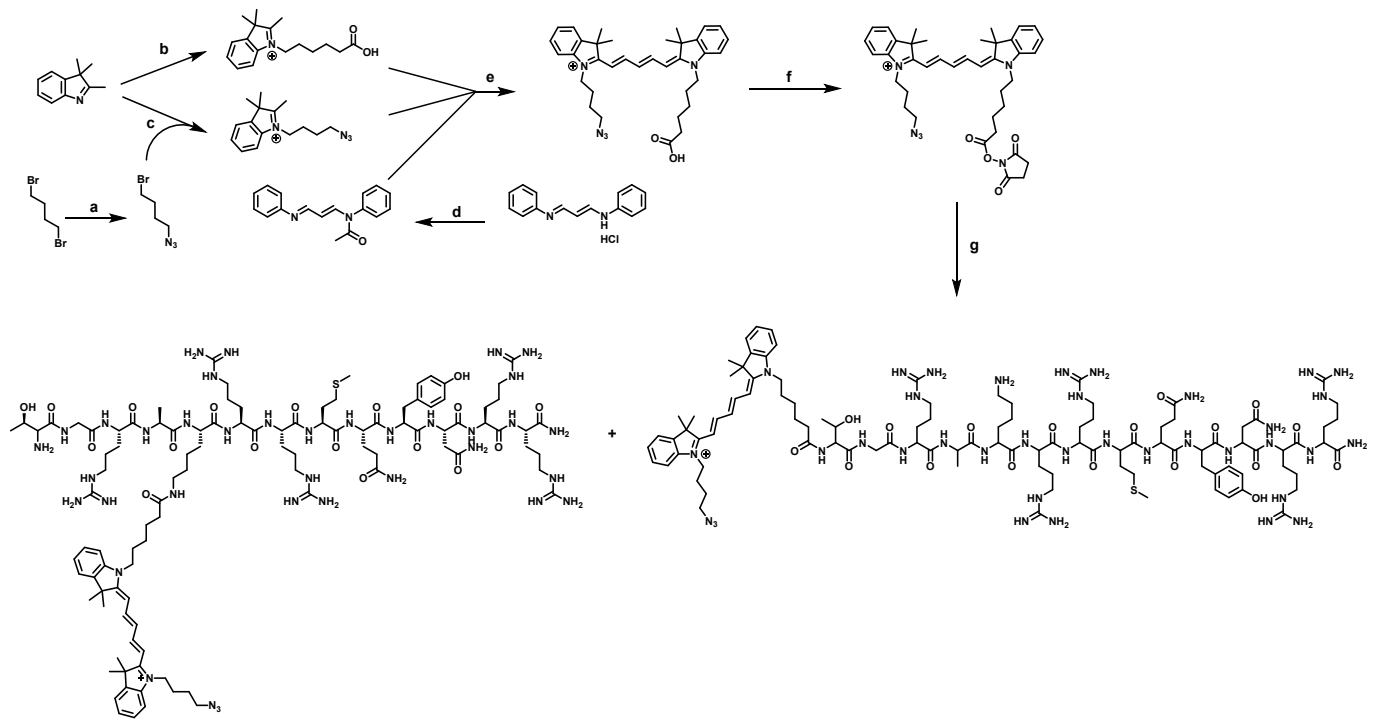


**Figure S2.** MALDI-TOF spectrum of 1-(4-azidobutyl)-2-((1E,3E)-5-((E)-1-(5-carboxypentyl))-3,3-dimethylindolin-2-ylidene)penta-1,3-dien-1-yl)-3,3-dimethyl-3H-indol-1-ium.

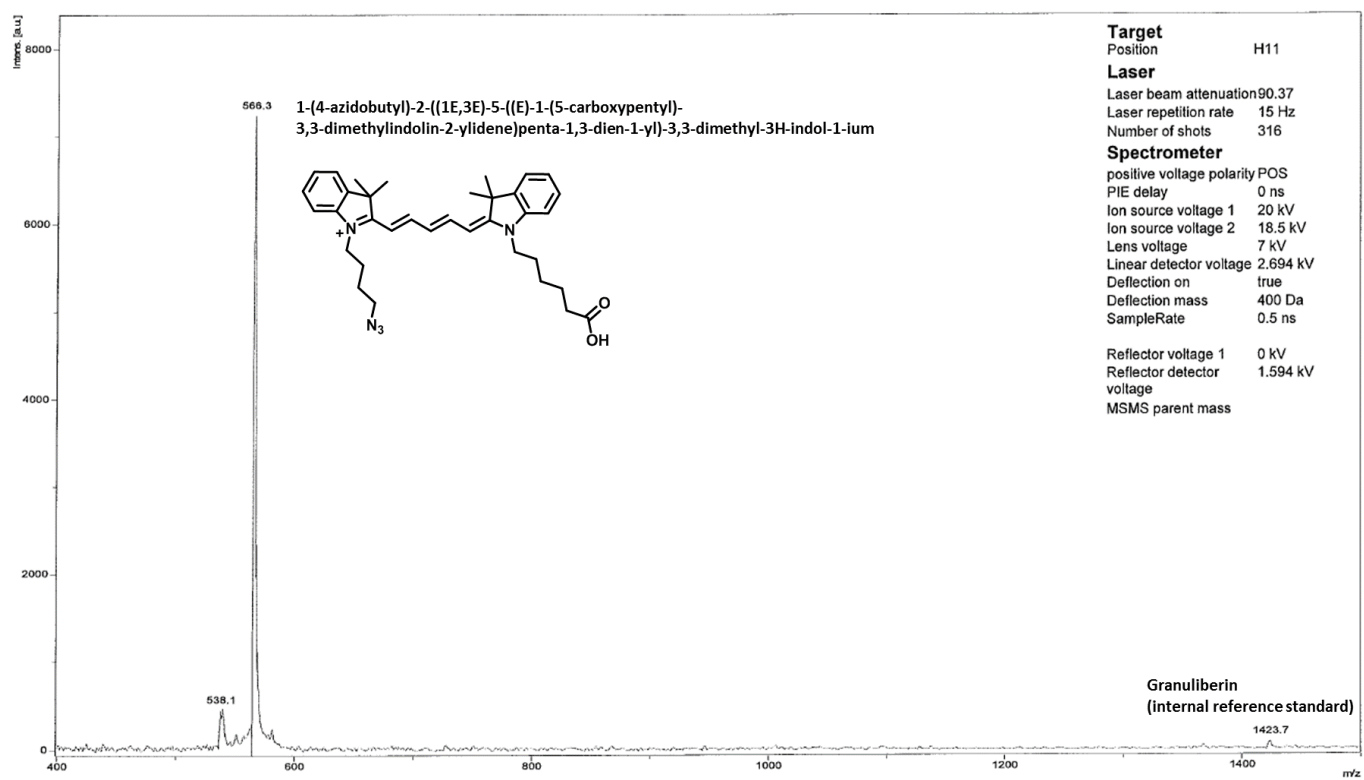


**Figure S3.** MALDI-TOF spectrum of 1-(4-azidobutyl)-2-((1E,3E)-5-((E)-1-(6-((2,5-dioxopyrrolidin-1-yl)oxy)-6-oxohexyl)-3,3-dimethylindolin-2-ylidene)penta-1,3-dien-1-yl)-3,3-dimethyl-3H-indol-1-i um.

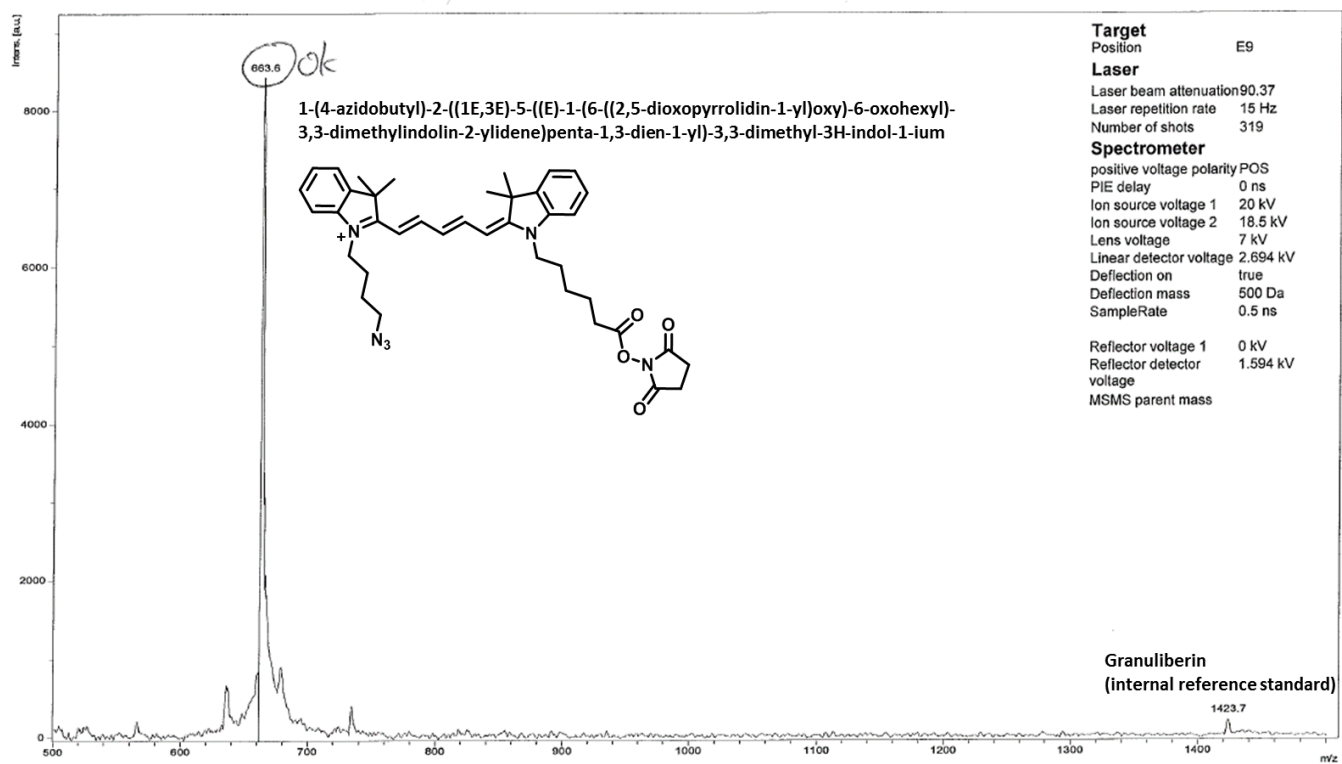


**Figure S4a.**  $^1\text{H-NMR}$  spectrum of 1-(4-azidobutyl)-2-((1E,3E)-5-((E)-1-(6-((2,5-dioxopyrrolidin-1-yl)oxy)-6-oxohexyl)-3,3-dimethylindolin-2-ylidene)penta-1,3-dien-1-yl)-3,3-dimethyl-3H-indol-1-ium.

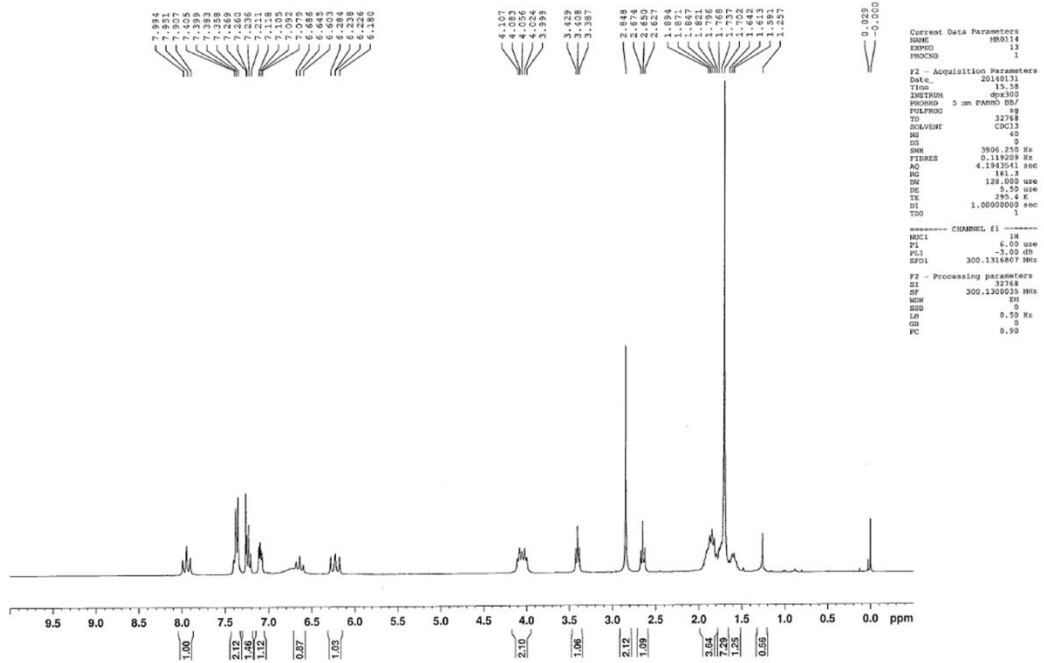


**Figure S4b.** Zoomed in on the aromatic peak area of the  $^1\text{H-NMR}$  spectrum of 1-(4-azidobutyl)-2-((1E,3E)-5-((E)-1-(6-((2,5-dioxopyrrolidin-1-yl)oxy)-6-oxohexyl)-3,3-dimethylindolin-2-ylidene)penta-1,3-dien-1-yl)-3,3-dimethyl-3H-indol-1-ium.

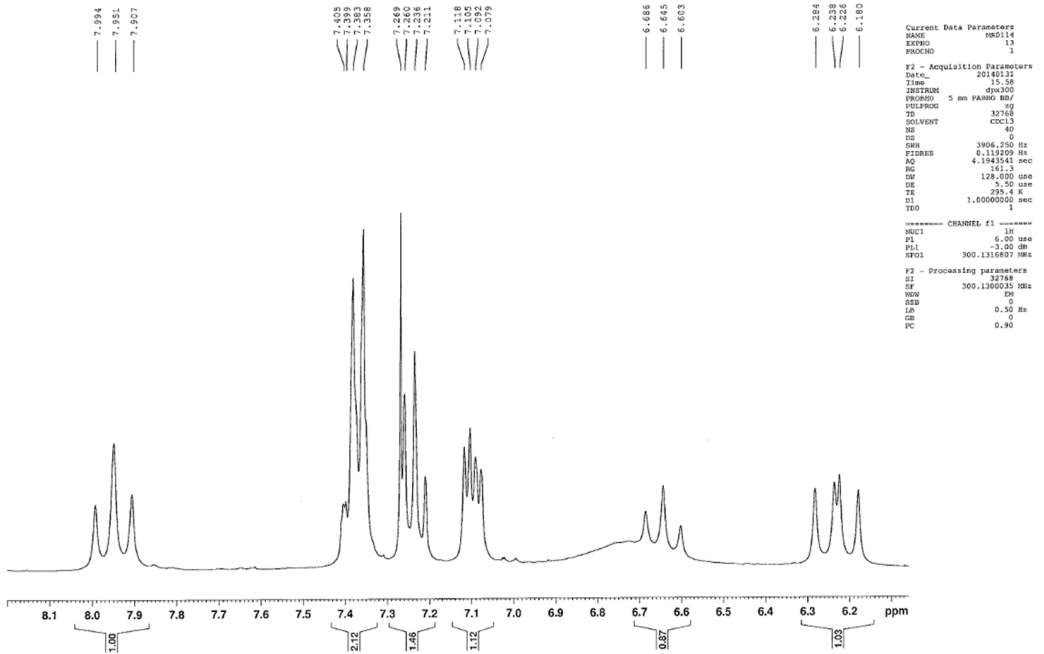


**Figure S5.** HPLC reverse-phase chromatography of the purification and characterization of  $\text{UBI}_{29-41}\text{-Cy5-N}_3$ . Chromatogram with the collected product peaks depicted by red arrow/lines.

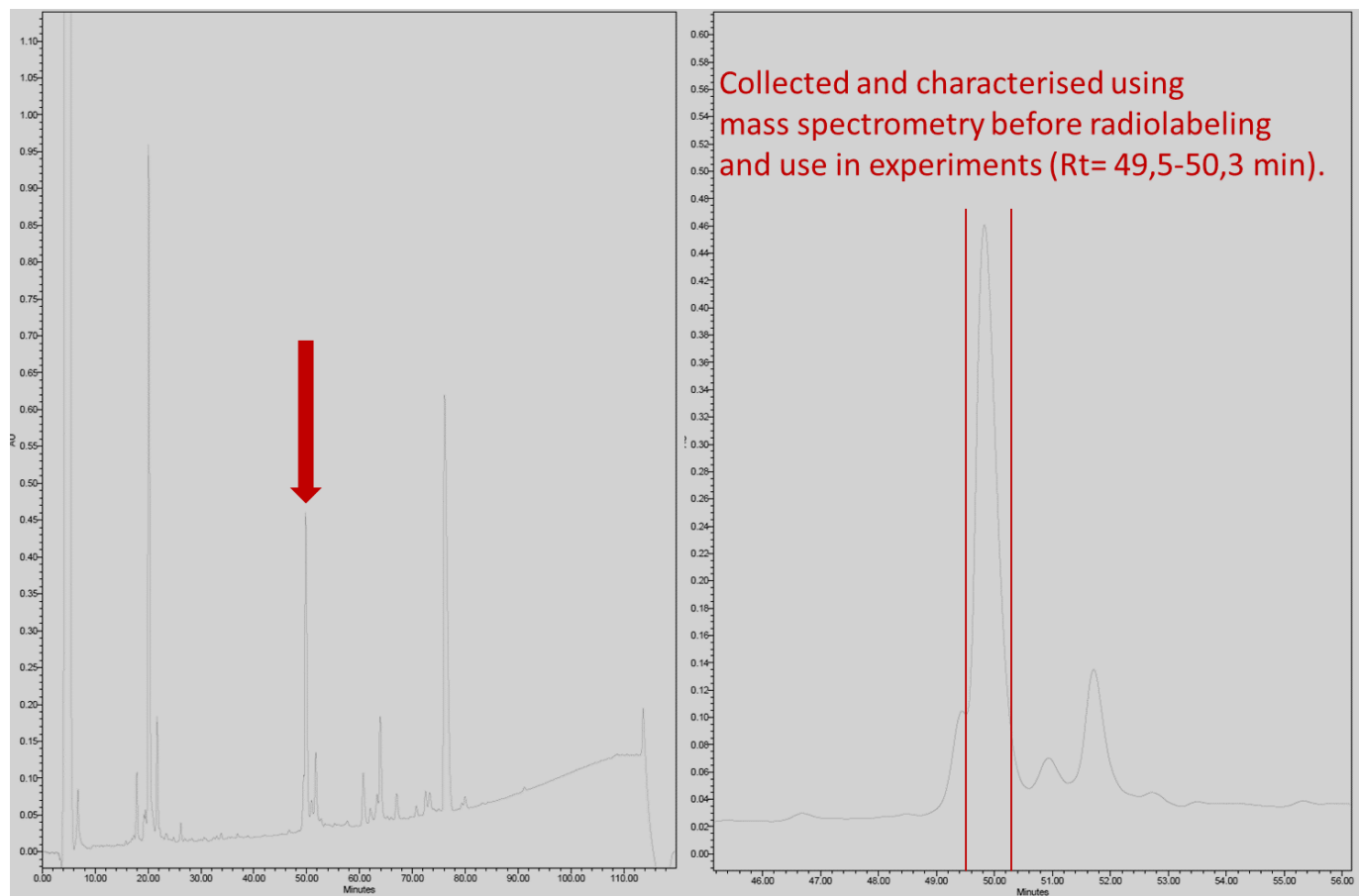


**Figure S6.** MALDI-TOF spectrum of HPLC purified UBI<sub>29-41</sub>-Cy5-N<sub>3</sub>. The red asterisk represents an alternative attachment point of the dye. This, however, will not change the recorded mass.

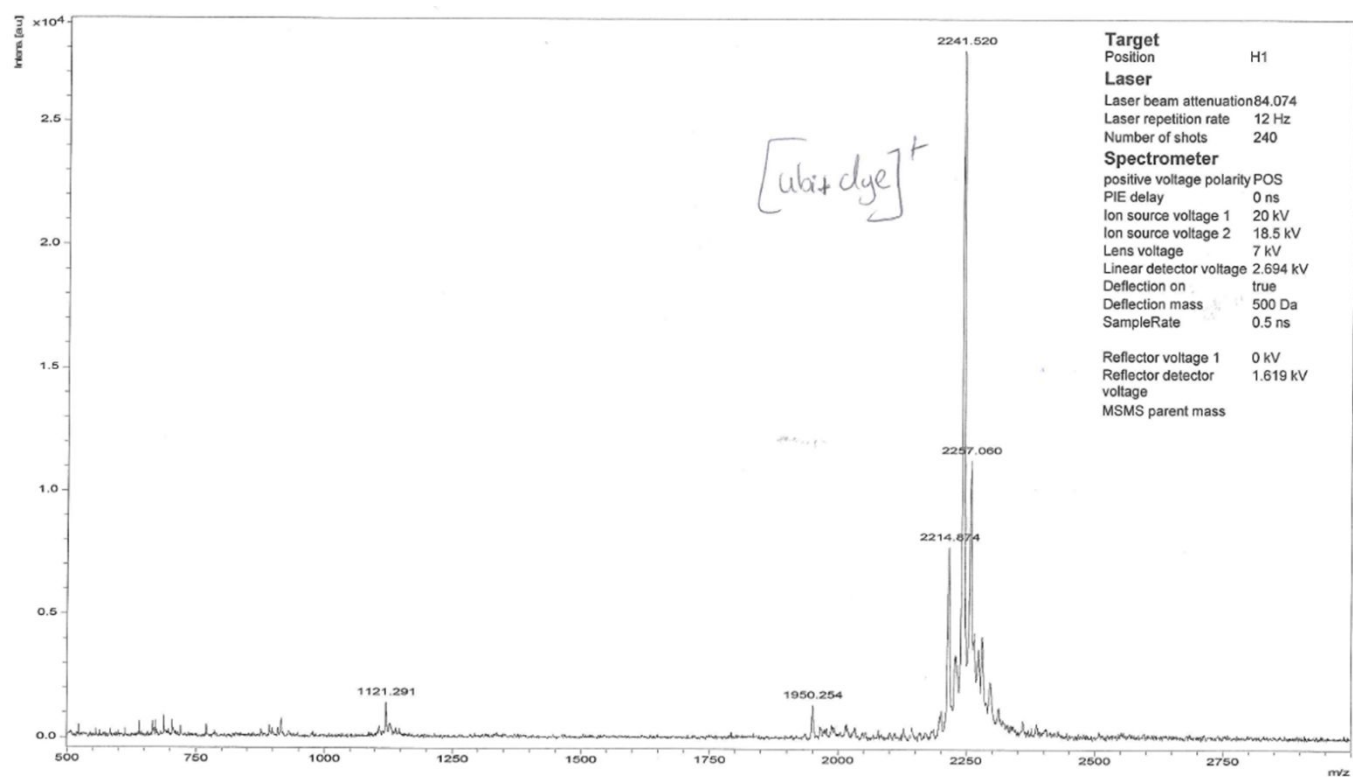


**Figure S7.** Schematic depiction of  $^{99m}\text{Tc}$  labeled UBI<sub>29-41</sub>-Cy5-N<sub>3</sub> according to Meléndez-Alafort *et al.* Nucl Med Biol. 2003;30(6):605. However, it is likely that other binding modes are also present in solution.

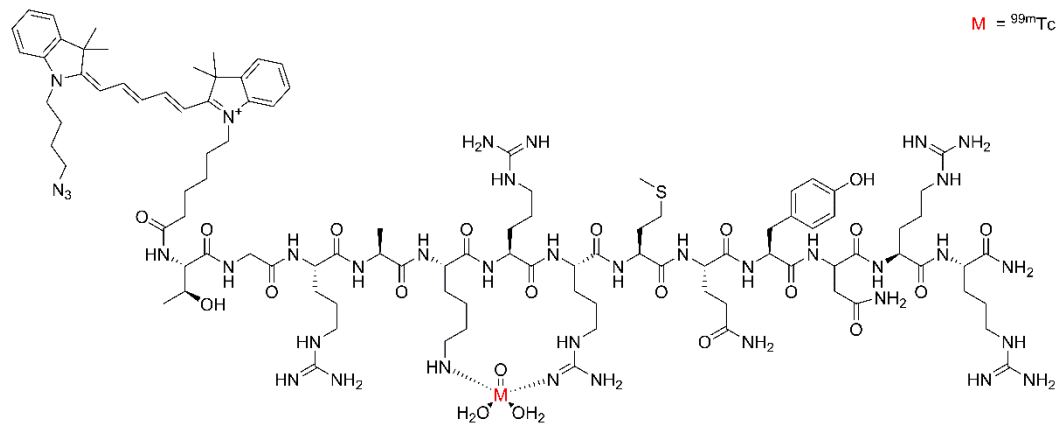


**Figure S8.** **A)** BHI agar plates containing serial dilutions of *S. aureus* from urine samples. **B)** assessment of viable bacteria in urine at various intervals after I.M. injection of  $1 \times 10^7$  CFU bacteria. Control = urine collected from non-infected mice. BDL = CFU's below detection limit. **C)** Radioactivity ( $^{99m}\text{Tc}$  expressed as %ID) and fluorescence (Cy5, expressed as Total Flux (p/s)/pixel) measurements in urine samples. Data are expressed as the mean of 3 observations. Error bars represent the standard deviation.

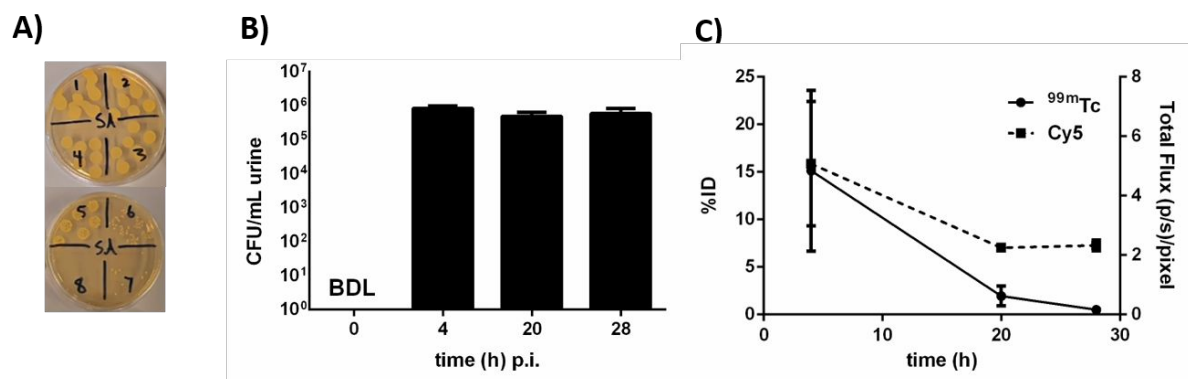


**Figure S9.** Confocal microscopic imaging of phagocytosis of UBI<sub>29-41</sub>-Cy5-N<sub>3</sub> labeled *S. aureus* by human macrophages. Images were taken at t = 0 (A), 6 (B), and 30 (C) min. A few examples are highlighted with arrows indicating free (white arrow) or phagocytosed (yellow arrow) *S. aureus*. Grey = bright field, blue = Hoechst, red = Cy5. D) = UBI<sub>29-41</sub>-Cy5-N<sub>3</sub> labeled dead *S. aureus*.

